Cytochemical Aspects of Cellulose Breakdown During the Infection Process of Rubber Tree Roots by *Rigidoporus lignosus*

Michel R. Nicole and Nicole Benhamou

Orstom–Forêts Canada, 1055 Rue du Peps, G1V 4C7 Sainte-Foy, Québec, Canada, and Département de Phytologie, Faculté des Sciences de l'Agriculture et de l'Alimentation, Université Laval, C1K 7P4 Sainte-Foy, Québec, respectively.

We thank M. Sylvain Noel and C. Moffet for skillful technical assistance, and G. B. Ouellette (Forêts Canada, Sainte-Foy, Québec) and R. A. Blanchette (University of Minnesota, St. Paul) for revising the manuscript.

Accepted for publication 26 June 1991.

ABSTRACT

Nicole, M. R., and Benhamou, N. 1991. Cytochemical aspects of cellulose breakdown during the infection process of rubber tree roots by *Rigidoporus lignosus*. Phytopathology 81:1412-1420.

An exoglucanase purified from a cellulase produced by the fungus *Trichoderma harzianum* was bound to colloidal gold and used for ultrastructural detection of cellulosic β-(1-4)-D-glucans in root tissues of rubber trees (*Hevea brasiliensis*) infected by the white rot root pathogen, *Rigidoporus lignosus*. Large amounts of β-1,4-glucans were found in cell walls of healthy roots, except in suberized walls that were not labeled. Gold particles were absent in the fungal wall inside rhizomorphs and in infected host cells. In infected roots, cell wall degradation occurred both close to and at a distance from hyphae, causing variable decaying patterns. Few gold particles or absence of labeling were observed in degraded phellem and phloem cell walls. In xylem vessel elements, labeling did not occur over incompletely digested areas of the S_2 layer of secondary walls. During pit penetration by hyphae, degraded primary walls and the S_1 layer of secondary walls were devoid of gold particles. The present cytochemical data provide evidence for cellulose degradation in roots of rubber trees infected by *R. lignosus*. They demonstrate indirectly the implication of cellulases in the decay process and give more insight into the role cellulose degradation plays in white rot pathogenesis by *R. lignosus*.

Additional keywords: lignin, suberin, tree-fungi interactions.

In recent years, infections of woody plants by white rot fungi that cause root rots have been the focus of considerable interest, mainly because of the importance that wood has gained in the economy of several tropical countries. In rubber tree-growing areas in West Africa (14), the white rot root of *Hevea brasiliensis* (Willd. ex Adr. Juss.) Müll. Arg. caused by the basidiomycete *Rigidoporus lignosus* (Klotzsch) Imazeki is considered to be one of the most destructive diseases and is responsible for yield losses up to 50% in the older plantations (30). The *H. brasiliensis-R. lignosus* interaction has been studied at both the light and electron microscope levels (35). Previous reports have stated that root infection proceeds by fungal penetration either through lenticels and/or wounds, or by means of a degradation process of the host cell surface (32,35). During pathogen ingress towards the vascular stele, severe host cell alterations occur, including marked cell wall degradation in both the phellem and the phloem as well as disintegration of lignin-rich primary and secondary walls of xylem vessel elements (35). In addition, it has been shown that phloem colonization leads to internal rubber coagulation, thus resulting in the cessation of latex yield (34).

As with other wood-decaying fungi, *R. lignosus* is capable of producing an array of lytic enzymes involved in the degradation of polymeric carbohydrates found in woody plant cell walls (22). Among the chain-splitting hydrolases that have been identified so far, cellulolytic enzymes are thought to play a major role during the infection process by facilitating host cell penetration and extensive tissue colonization (21,27). Oxidases such as laccases, related to the infection process (20,22), and an Mn-peroxidase, only characterized in vitro (19), also may contribute to cell wall biodegradation by their harmful action on lignin (20). Although standard electron microscopy and biochemical investigations of infected roots of *H. brasiliensis* have undoubtedly contributed to the unraveling of some mechanisms related to the deleterious action of *R. lignosus,* data at the molecular level in planta are still lacking. Advent of modern cytochemical techniques in plant pathology recently has opened new avenues for accurately localizing cell surface molecules (2,5). In particular, such approaches have been useful for studying cellulose distribution in cell walls of plants infected by vascular pathogens (4,11), inert wood fragments attacked by microbial degraders (8), and interfacial materials formed in mycorrhizal plants (10). By taking advantage of the availability of a specific probe for cellulose localization (2–4), our objective was to complement earlier ultrastructural observations on *R. lignosus*-infected rubber tree root tissues by a cytochemical analysis of cellulose distribution during infection and colonization, including xylem decay. In the present paper, particular attention has been paid to the extent of host wall degradation by cellulolytic enzymes produced by this root-rotting fungus during wood colonization (21,22).

MATERIAL AND METHODS

Fungal culture and growth conditions. Isolates of *R. lignosus* were collected from infected rubber trees grown on Ivory Coast plantations. The mycelium was obtained by growing *R. lignosus* strain 1 on a 2% malt agar medium (Difco, Detroit, MI) at 28 C.

Artificial inoculations of plant material. Seeds of rubber tree,

clone GT 1, were collected in a plantation of the Institut de Recherche du Caoutchouc of Ivory Coast (IRCA). After germination in sand, young seedlings were transferred to tubs (10 × 1 × 1 m) filled with forest soil, the moisture content of which was monitored by watering to saturation and controlled with a neutronic moisture gauge (Solo 20, Nardeux, France). Seedling inoculation was performed as previously described (29). Briefly, five preinfected rubber wood fragments were applied against the taproot of each 1-mo-old seedling at a depth of 20 cm in the soil. Root samples were collected at 2, 4, 10, and 15 wk after inoculation. Noninfected plants were used as controls.

Tissue processing for transmission electron microscope (TEM) observations. Infected roots were fixed in toto for 1 h in 3% glutaraldehyde (v/v) in 0.1 M sodium cacodylate buffer, pH 7.2. Small root fragments then were excised, fixed again for 1 h with 3% glutaraldehyde, postfixed with 1% osmium tetroxide in the same buffer for 1 h at 4 C, and washed in sodium cacodylate buffer before dehydration in a graded ethanol series. They then were embedded in Epon 812 or in Araldite. Ultrathin sections, collected on Formvar-coated nickel grids (200 mesh), were processed for cytochemical labeling. Observations were carried out with a JEOL 1200 EX electron microscope operating at 80 kV.

Three to five samples per infected root were examined. Samples from healthy rubber tree roots were processed as mentioned above and used as controls.

Enzyme. The exoglucanase used in this study, a β-(1-4)-D glucan cellobiohydrolase (EC 3.2.1.91), was purified in a five-step procedure from a cellulase produced by the cellulolytic fungus *Trichoderma harzianum* Rifai (4). The exo β-(1-4) glucanase activity was tested against Avicel and carboxymethylcellulose (Sigma, St. Louis, MO). It was determined to be 20 U/mg; 1 unit was the amount of enzyme needed to liberate reducing sugars equivalent to 0.55 μM glucose per minute under the assay conditions (2). The pH of optimal activity of the enzyme was estimated to be 5.0–5.6 and its molecular weight was 64 Kd.

Preparation of the enzyme-gold complex. Colloidal gold (Sigma) with particles averaging 15 nm in diameter was prepared according to Frens (18). Ten milliliters of the gold suspension, adjusted to pH 9.0 (isoelectric point of the enzyme) with 0.2 M K_2C0_3, was added to 1 mg of purified exoglucanase dissolved in 0.2 M phosphate-buffered saline (PBS), pH 7.4. The mixture was centrifuged at 25,000 rpm with a Ti 50 rotor for 45 min. The red mobile pellet was recovered in 0.5 ml of 0.2 M PBS, pH 6.0, containing 0.02% of polyethylene glycol (PEG) 20,000.

Cytochemical labeling. Sections of infected and healthy root samples were first floated on a drop of PBS-PEG, pH 6.0, and incubated on a drop of the enzyme-gold complex for 30 min at room temperature in a moist chamber. They then were thoroughly washed with PBS, pH 7.4, rinsed with distilled water, and finally contrasted with uranyl acetate and lead citrate before examination.

Cytochemical controls. Specificity of labeling was assessed by means of the following control tests: incubation with the exoglucanase-gold complex to which 5 mg of β-(1-4)-D-glucans was previously added; incubation with a bovine serum albumin (BSA)-gold complex, a nonenzymic protein-gold complex; and incubation of uninoculated healthy plants.

RESULTS

Labeling pattern observed in healthy roots. Following incubation of ultrathin sections of uninoculated root tissues with the exoglucanase-gold complex, an intense and regular labeling occurred over cell walls of most tissues except the phellem, where gold particles were unevenly distributed. All other structures, including organelles, cytoplasm, and plasma membrane, were free of significant labeling.

Walls of dead surface cells of the rhytidome were labeled regularly. In the phellem, cell walls were labeled unevenly: the outermost highly suberized part adjacent to the middle lamella was nearly unlabeled, whereas the nonsuberized innermost fraction was labeled regularly (Fig. 1A). Both layers were of inequal thickness in adjacent cells. Numerous gold particles were found to be associated with the middle lamella adjacent to phellem cells. A heavy deposition of gold particles occurred over primary walls of phloem cells such as sieve tubes and latice vessels (Fig. 1B), but very little labeling occurred over the middle lamella. In the xylem, vessel cell walls also were intensively labeled (Fig. 1C), while the electron-opaque middle lamella and pit membranes were more slightly labeled.

All control tests, including incubation of sections with the exoglucanase-gold complex to which was previously added an excess of β-1,4-glucans from barley, yielded negative results (Fig. 1D).

Ultrastructural features of infected *H. brasiliensis* root tissues. Rhizomorphs of *R. lignosus* grew along the external surface of taproots (Fig. 2B) and produced infectious hyphae that penetrated outer root tissue through lenticels and wounds (Fig. 2D). During this early stage of infection, cell walls of hyphae showed considerable morphological changes because only thin-walled hyphae penetrated the root tissues. Pathogen ingress through the rhytidome proceeded by both inter- and intracellular modes of growth (Fig. 2C). In roots where dead surface cells were apparently missing, hyphae were closely appressed against the outermost cell layer of the phellem (Fig. 2B) and were capable of growing intramurally. Colonization of the vascular stele occurred via infection of parenchyma rays. Although phloem wall degradation was observed in all types of cells (Fig. 3B), hyphae were seldom seen in sieve tubes and never found in latice vessels. In contrast, xylem elements were extensively colonized. Invasion of these cells occurred often directly through the middle lamellae and pit membranes (Fig. 3C–F). Degradation of lignified secondary walls also was noticeable and appeared to result from the sequential alteration of the S_1, S_2, and S_3 layers of secondary walls.

Labeling pattern observed in infected roots. Two weeks after inoculation, rhizomorphs growing along the root surface were composed of numerous hyphae, the walls of which varied in texture and thickness (Fig. 2A). Following incubation of sections with the exoglucanase-gold complex, no labeling was seen over these laminated fungal walls (Fig. 2A). Similarly, gold particles were absent over the amorphous interhyphal-connecting material as well as over the interfacial material between host and fungus (Fig. 2B). At points of fungal penetration, wall degradation of dead surface cells was restricted to the channel of penetration as judged by the regular distribution of gold particles along the fungus pathway (Fig. 2C). In areas where rhizomorphs established direct contact with phellem cell walls, a local alteration of host walls was observed (Fig. 2D). Hyphae also invaded junctions between nonlabeled, suberized areas and highly labeled areas of phellem cell walls. Few gold particles were noticeable in areas close to hyphae (Fig. 2E).

About 4 wk after inoculation the fungus reached the phellem, causing extensive tissue degradation and cell wall breakdown. Cell wall degradation was severe and concerned both suberized and nonsuberized fractions. Incubation of sections with the exoglucanase-gold complex revealed that gold particles were absent over areas adjacent to the channel of hyphal penetration (Fig. 4A). At a distance from the point of fungal penetration, some apparently altered wall areas also were nearly devoid of labeling (Fig. 4B). At a more advanced stage, the penetration area was completely digested (Fig. 4C). No gold particles could be detected in the middle lamella. Alteration of suberized walls at a distance from pathogen penetration occasionally was observed (Fig. 4D–E). Breakdown of the middle lamella caused the splitting of adjacent suberized walls, which were damaged in front of the penetrating hyphae (Fig. 4E). When hyphae moved into the middle lamella, digestion took place around the fungus. The degraded zones were devoid of gold labeling (Fig. 4F, thick arrows). Advanced stages of phellem colonization resulted in extensive wall decay (Fig. 4G) since extensive amounts of wall material were removed. Large digested areas were free of labeling. Few gold particles were observed on residual fibrillar material only.

During fungal ingress, which coincides to about 10 wk after inoculation, hyphae of *R. lignosus* were mainly observed in

parenchyma rays, seldom in sieve tubes, and never in latice vessels in which rubber particles were produced. In spite of this slight colonization, walls of all phloem cells could be seriously damaged. Incubation of sections with the exoglucanase-gold complex revealed that apparently altered wall areas were slightly labeled (Fig. 3A). Cell walls and middle lamellae could be attacked simultaneously; erosion then extended locally toward secondary walls, over which unlabeled areas were noted (Fig. 3B). In the degraded areas, gold particles only occurred over residual fragments.

At 15 wk after inoculation, hyphae of *R. lignosus* were widespread in xylem cells. Cell wall alteration occurred either close to hyphae or at a distance from them. Colonization mainly proceeded through pit membrane penetration and middle lamella breakdown. Cytochemical investigation of β-(1-4)-D-glucans revealed that gold particles were absent in the altered wall during the early stage of pit membrane penetration (Fig. 3C and D), mainly close to the hyphae. Gold particles were irregularly distributed in degraded wall areas localized in the S_1 layer of secondary walls (Fig. 3D). When pit penetration was achieved (Fig. 3E), unlabeled wall areas were seen along the fungal pathway (Fig. 3F). Few gold particles were observed in areas of the S_3 layer of secondary walls (Fig. 3F). When hyphae filled intercellular spaces, labeling of adjacent host cell walls varied according to wall degradation patterns (Fig. 5A).

Direct penetration of primary cell walls from cell lumens resulted in borehole formation through which the fungus moved. Wall alteration was thus mainly restricted along and in front of the fungus (Fig. 5B). Gold labeling was absent in some areas close to hyphae (i.e., in S_1 and S_2 layers of secondary walls and in primary walls). In front of penetrating hyphae, large unlabeled granular areas were found in the S_2 layer of the adjacent secondary cell wall. Few labeled fibers were seen that surrounded this area (Fig. 5B).

Major wall alterations also were noted in areas located away from hyphae. Very few gold particles were observed in the degraded areas of the S_1 layer of secondary walls. Disorganization of primary walls and of the S_1 layer of secondary walls resulted in the formation of decayed zones in which few gold particles were localized (Fig. 5C). A low amount of gold particles also was observed in the electron-dense areas of the S_2 layer of secondary walls (Fig. 5C). Similarly, degradation of pits occurred without hyphal contacts.

DISCUSSION

Our cytochemical results confirmed that in healthy roots of young rubber trees, cellulose occurred within cell walls of all root tissues. However, suberized portions of phellem cell walls were unlabeled after incubation with the enzyme-gold complex. This may be interpreted as indicating that suberization (deposition

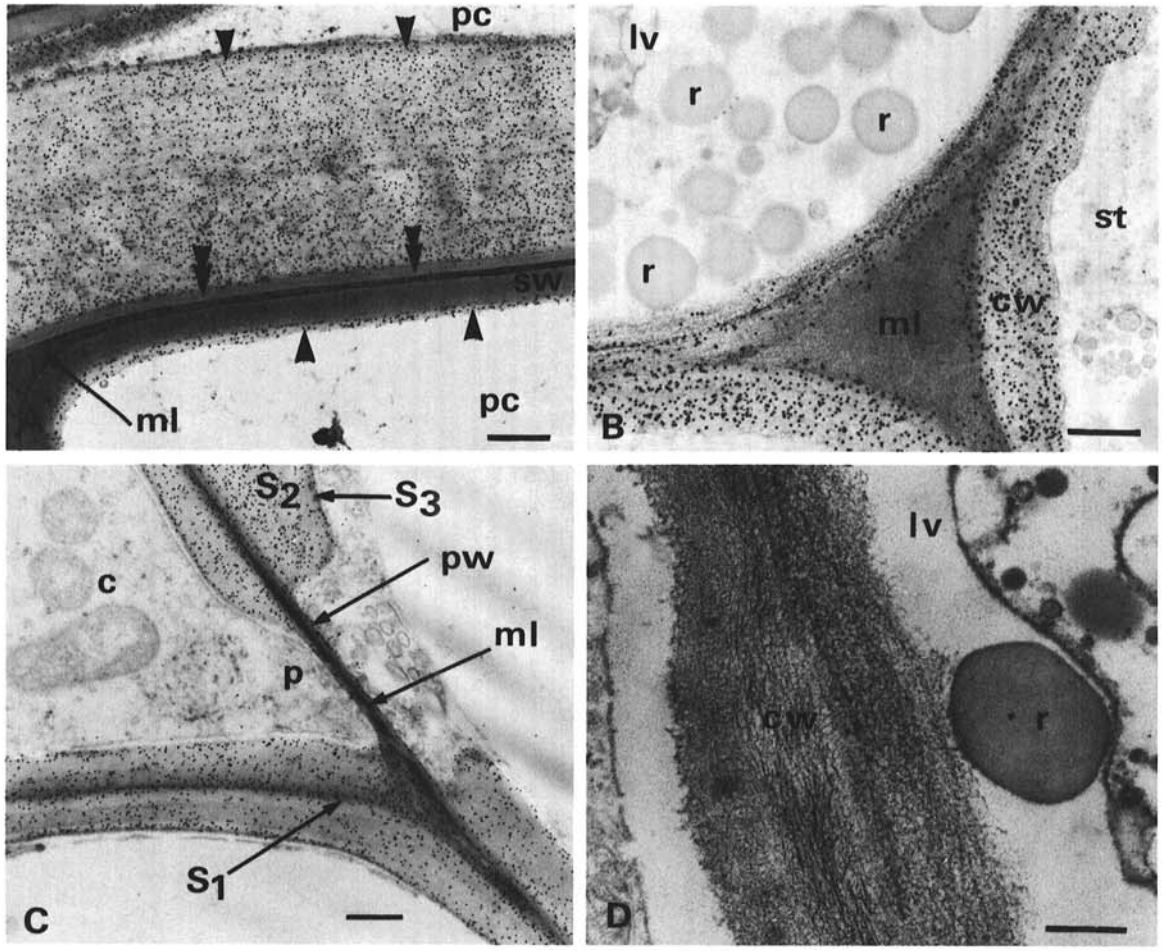

Fig. 1. TEM micrographs of healthy rubber tree roots fixed with glutaraldehyde and osmium tetroxide. **A–C,** Sections were treated with the exoglucanase-gold complex; **D,** sections were treated with the exoglucanase-gold complex previously incubated in a saturated solution of β-(1-4)-D-glucans as a control. **A,** Cell walls of the phellem. A large number of gold particles are associated with the innermost part of phellem cell walls (arrowheads). In contrast, the outermost part of walls that are suberized is never or rarely labeled (double arrowheads). The middle lamella also is slightly labeled. **B,** Cell walls of the phloem. Cellulosic walls of phloem cells (i.e., walls of sieve tubes or latice vessels containing rubber particles) are rich in gold particles, whereas the middle lamella is slightly labeled. **C,** Cell walls of the xylem. A regular distribution of gold particles occurs over the different layers of secondary walls. Pit membranes, primary walls, and middle lamellae are less labeled. **D,** No gold particles are visible in the cellulosic wall; gold deposition is strongly inhibited. c, Cytoplasm; cw, cell wall; lv, latice vessels; ml, middle lamella; p, pit membrane; pc, phellem cells; pw, primary wall; r, rubber particles; st, sieve tubes; sw, suberized wall; S_1, S_2, S_3, secondary wall layers. Bars = 0.5, 0.4, 0.5, and 0.2 μm for A–D, respectively.

of long chain fatty acids linked to a ligninlike polymer; 26) of originally cellulose-rich walls prevented accessibility of the gold-complex probe to its corresponding receptor sites. In many tree species, the phellem consists of cork cells and of nonsuberized cells called phelloid cells (17). In contrast, in young rubber tree roots, walls of all phellem cells are made of both suberized and nonsuberized portions; the outermost part, adjacent to the middle lamella, is thought to be highly suberized whereas the inner frac-

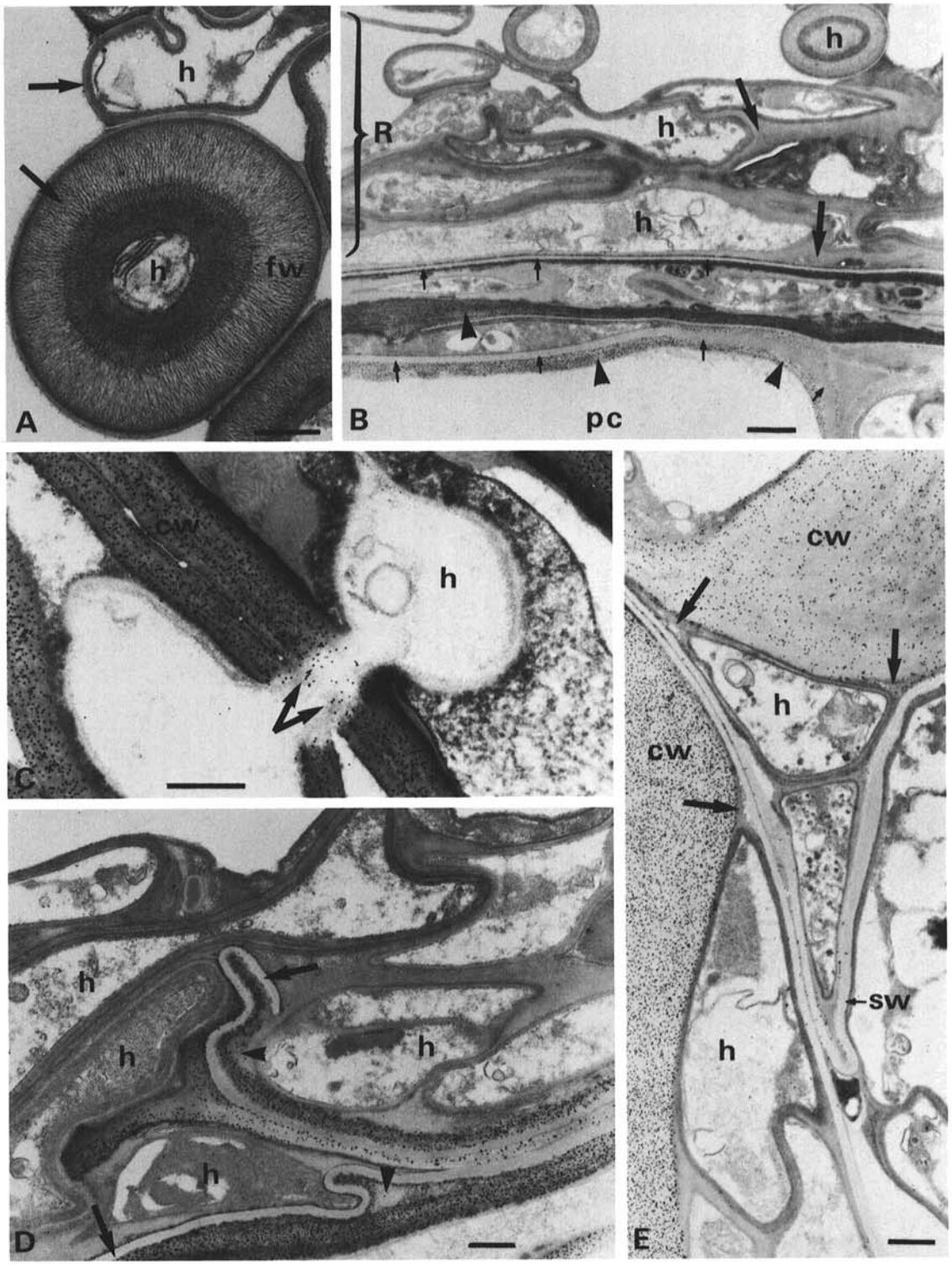

Fig. 2. TEM micrographs of *Rigidoporus lignosus*-infected rubber tree roots fixed with glutaraldehyde and osmium tetroxide. Sections were treated with the exoglucanase-gold complex. **A–B,** Rhizomorphs growing along the root. **A,** Several hyphae with variable cell wall thickness (arrows). No gold particles are found over the fungal cell wall. **B,** Dead surface cells are locally removed from the root surface; rhizomorphs are in contact with the outer phellem cell layers. Hyphae of rhizomorphs are gathered in an unlabeled mucilagelike substance (thick arrows). Thin arrows indicate suberized walls that are unlabeled; in contrast, the innermost part of cell walls (arrowheads) is rich in gold particles. **C–E,** Fungal penetration in roots. **C,** Wall penetration of dead surface cells. Digestion of walls of dead surface cells by a penetrating hypha; few gold particles are seen along the fungal neck (arrows). **D,** Early stage of fungal penetration in roots. No gold particles are visible in the outer suberized cell wall layer of phellem cells (arrows). Close to hyphae, small areas in the cell wall are devoid of gold particles (arrowheads). **E,** Hyphal penetration through junctions between unlabeled suberized walls and labeled walls of the outer cell layer of the phellem. A slight digestion of cell walls (arrows) occurs close to hyphae; the amount of gold particles is low in these degraded areas. cw, Cell wall; fw, fungal cell wall; h, hyphae; pc, phellem cells; sw, suberized wall; R, rhizomorphs. Bars = 0.4, 1, 0.4, 0.5, and 0.5 μm for A–E, respectively.

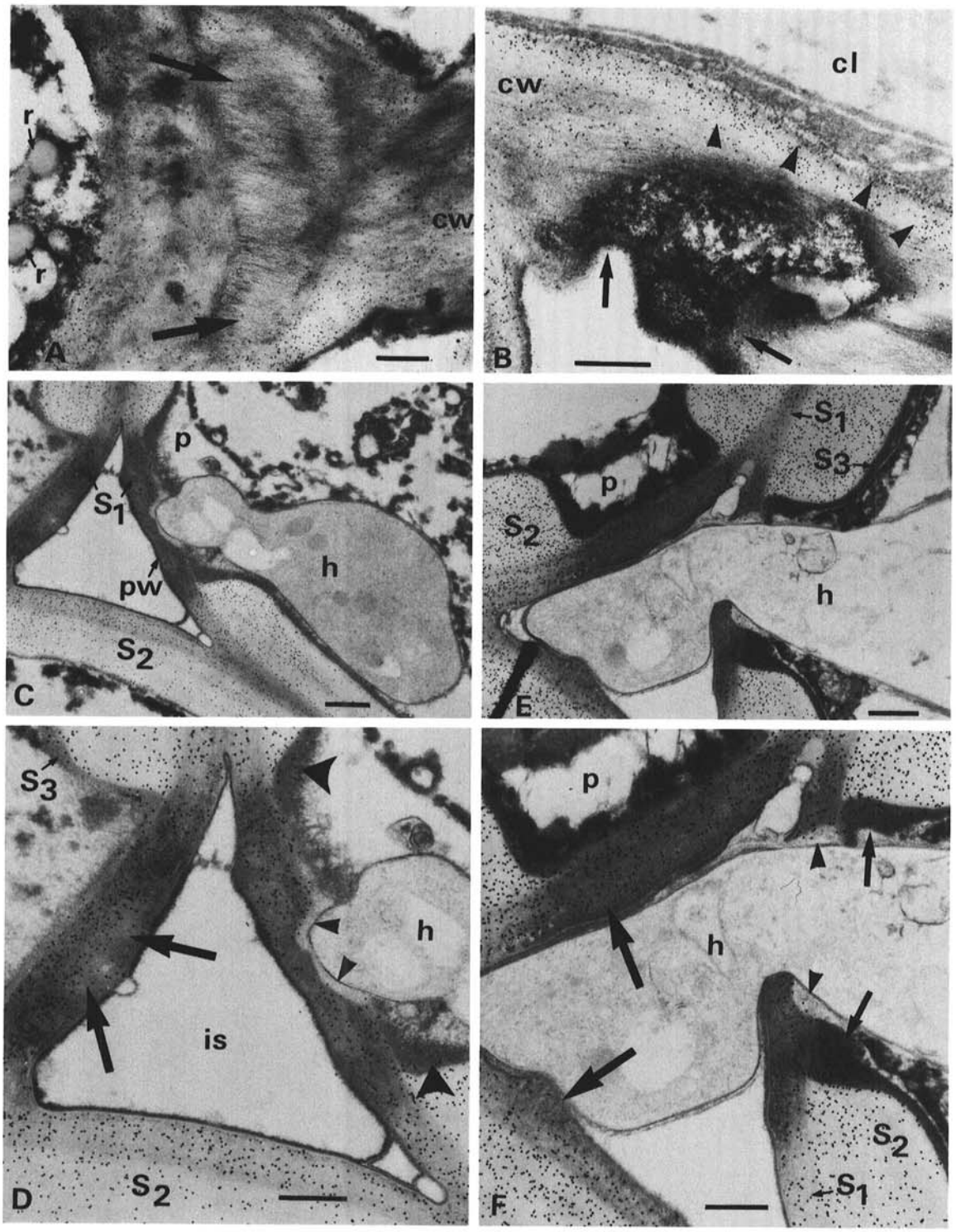

Fig. 3. TEM micrographs of phloem and xylem cell wall degradation by *Rigidoporus lignosus* in rubber tree roots fixed with glutaraldehyde and osmium tetroxide. Sections were treated with the exoglucanase-gold complex. **A** and **B,** Cell wall labeling in the infected phloem. **A,** Large fibrillar areas of latice vessel walls are devoid of gold particles (arrows). **B,** The degraded wall is highly electron-dense (arrows); few gold particles are localized over the eroded wall. Erosion seems to progress toward cell lumen (arrowheads) of nearby parenchyma cells. **C–F,** Cell wall labeling in infected xylem. **C,** Early stage of pit cell wall penetration. A fungal cell begins penetrating a pit membrane. The primary wall and the S_1 layer of the secondary wall are more electron-dense than the other cell wall layers. **D,** Enlargement of **C.** No labeling occurs over degraded areas of the secondary wall S_1 layer close to the hypha (small arrowheads). On the other side of the intercellular space, the primary wall and the S_1 layer are digested; few gold particles are seen in these degraded areas (arrows). Accumulation of dense material is visible along the S_3 layer and in the pit area (large arrowheads). **E,** Advanced stage of pit cell wall penetration. The hypha fills the intercellular space after it degraded the pit membrane. **F,** Enlargement of **E.** Unlabeled material remains along the fungal cell (arrowheads). A low concentration of gold particles can be seen over primary walls and the secondary S_1 layer close to the hypha (large arrows), whereas regular gold labeling is evident in the undegraded S_2 layer. Few gold particles also are visible over the dense material in the pit area (small arrows). cl, Cell lumen; cw, cell wall; h, hyphae; is, intercellular space; p, pit membrane; pw, primary wall; r, rubber particles; S_1, S_2, S_3, secondary wall layers. Bars = 0.5, 0.5, 0.5, 0.4, 0.5, and 0.4 μm for A–F, respectively.

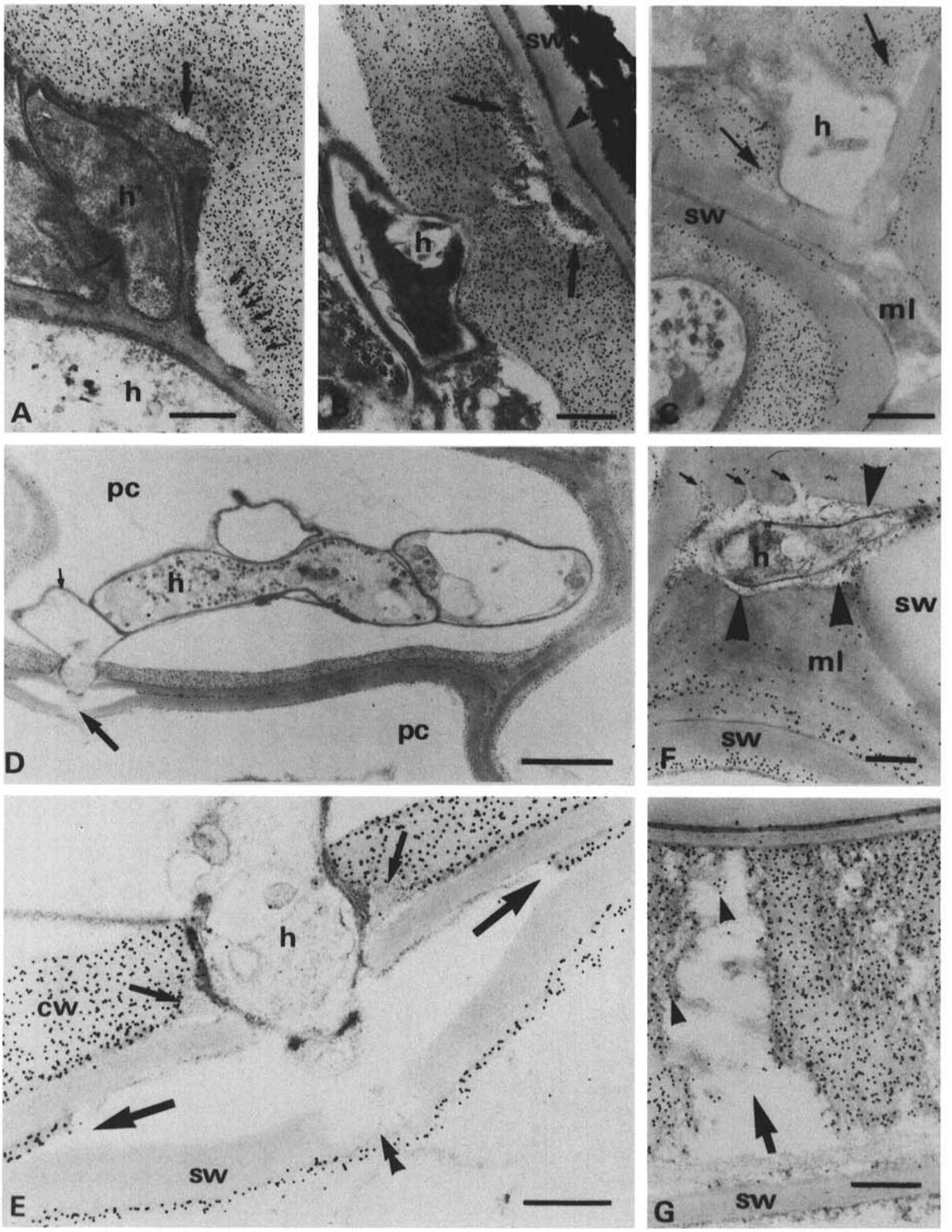

Fig. 4. TEM micrographs of phellem cell wall degradation by *Rigidoporus lignosus* in rubber tree roots fixed with glutaraldehyde and osmium tetroxide. Sections were treated with the exoglucanase-gold complex. **A,** No gold particles are found in degraded areas close to the fungus at a wall penetration site (thick arrow). A small amount of gold particles can be seen in the degraded cell wall located near the outward progression of erosion (thin arrows). **B,** An advanced stage of phellem cell wall penetration. Wall degradation (unlabeled) occurs at a distance from the fungus (arrows). A few gold granules are seen over the degraded middle lamella (arrowhead). **C,** A microhypha achieves cell wall penetration. No gold particles are distinguishable along the fungal tip (arrows). The degraded middle lamella also is unlabeled. **D,** Localization of the fungus in phellem cells. A fungal cell (small arrow) has penetrated both labeled cell wall layers and unlabeled suberized layers (large arrow). **E,** Portion of **D** showing host cell wall penetration by the pathogen. Degraded host cell wall areas are devoid of gold particles (small arrows). Middle lamella close to the hyphal tip is removed (large arrows), causing the separation of suberized layers of adjacent phellem cell walls. In addition, extensive suberin digestion occurs in front of the hyphal tip (double arrowheads). **F,** Well-delineated areas of digested middle lamella (arrowheads) characterized by the absence of gold particles close to the hypha. Degradation of the middle lamella also occurs at a distance from the fungus (small arrows). **G,** An advanced stage of decay in phellem cells characterized by large degraded wall areas (arrow). Only few gold particles are visible in the digested area (arrowheads). cw, Cell wall; h, hyphae; ml, middle lamella; pc, phellem cells; sw, suberized walls. Bars = 0.4, 0.5, 0.5, 1.5, 0.4, 0.4, and 0.4 μm for A–G, respectively.

tion is likely cellulosic. Such an organization was found to occur in 12-mo-old trees.

Colloidal-gold labeling of sections from tissues collected during the early process of root penetration by hyphae showed that cell walls of *R. lignosus* were free of cellulose, unlike some other phytopathogenic fungi (2). Morphological alterations concerning fungal wall thickness during root penetration may be related to changes in wall components such as chitin and β-(1-3)/(1-6)-

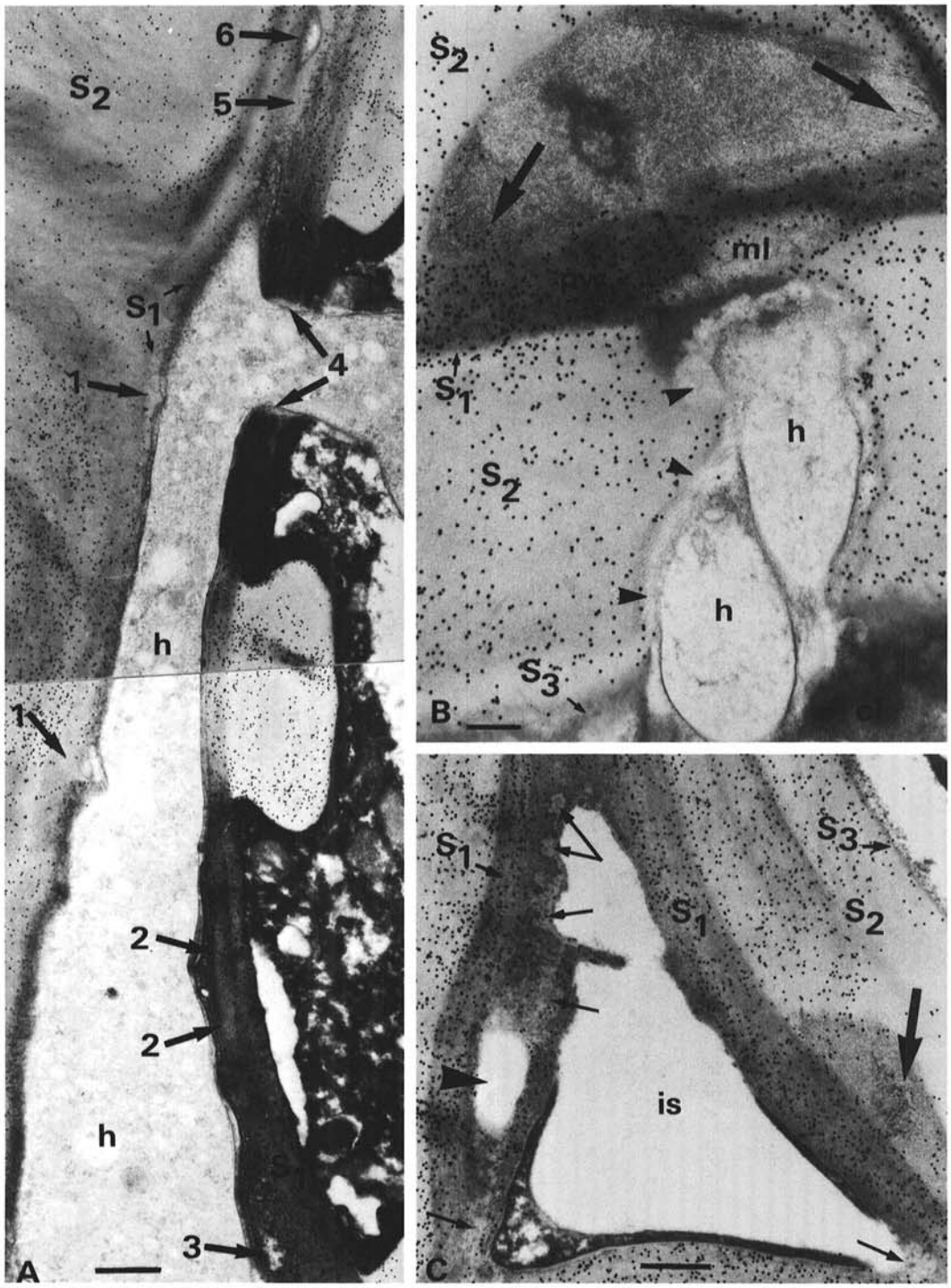

Fig. 5. A–C, TEM micrographs of *Rigidoporus lignosus*-infected xylem in rubber tree roots fixed with glutaraldehyde and osmium tetroxide. Sections were treated with the exoglucanase-gold complex. **A,** A fungal hypha fills the intercellular space between xylem cells. Numerous gold particles are seen in the nondegraded walls. Different patterns of labeling are noticeable in relation to wall digestion. 1) Few gold particles occur in slightly degraded primary wall and S_1 layer of the secondary wall close to the hypha. 2) Before digestion, granular areas were seen in the S_1 layer of the secondary wall, in which concentration of gold particles is extremely low. 3) No gold particles are detected in the degraded S_1 layer. 4) Unlabeled areas are seen over the eroded pit membrane close to the fungal neck. 5) Disorganized S_1 layer of the secondary wall and the primary wall do not exhibit gold binding. 6) Complete degradation of the S_1 layer of the secondary wall in which gold particles are absent. **B,** Borehole formation by microhyphae through a xylem vessel wall. Degraded areas of the layers of the secondary wall along the fungal pathway are devoid of gold particles (arrowheads). In front of the hypha, a large underlying and unlabeled zone is visible; it is bordered with fibers over which some gold particles are noticeable (arrows). The electron-dense primary wall and the middle lamella also are less labeled. **C,** Degradation of intercellular space borders without contact with the pathogen. Unlabeled cavities are localized in primary walls and in the S_1 layer of secondary walls (thin arrows). No gold particles are seen in the completely degraded S_1 layer of the secondary wall (arrowhead). An electron-dense area of the S_2 layer in the secondary wall is nearly free of gold particles (large arrow). cl, Cell lumen; h, hyphae; is, intercellular space; ml, middle lamella; pw, primary wall; S_1, S_2, S_3, secondary wall layers. Bars = 0.5, 0.2, and 0.4 μm for A–C, respectively.

glucans, which are ubiquitous polysaccharides in higher fungi (1).

Labeling of sections from *R. lignosus*-infected roots indicated that cellulose was altered in phellem, phloem, and xylem cell walls. Although it is considered that *R. lignosus* is mainly a lignin-degrading pathogen (22), this fungus degrades appreciable amounts of cellulose as judged by the decrease of labeling in degraded walls. Ultrastructural observations of ultrathin sections of infected roots revealed that cell wall alteration occurred at a distance from hyphae, suggesting that cellulose-degrading enzymes are able to diffuse in advance from the fungus. They probably act in conjunction with other hydrolases (i.e., pectinases and esterases) involved in middle lamella and suberin degradation, respectively (32); they also may be dependent on the action of lignin-degrading enzymes. Plant infection only begins when fast-growing rhizomorphs do not find any external food supply (31); breakdown products released from cellulosic cell walls may be an appropriate carbon source for *R. lignosus* before it reaches its lignin target. In addition, successful colonization of nonlignified tissues might be related to the action of cellulose-degrading enzymes. Phenol accumulation and/or defense lignification, which occur normally in infected rubber tree roots (33), are known to repress cellulase expression. Fungal laccases, secreted in the early stage of root penetration in young rubber trees (M. Nicole, *unpublished data*), may play a role in the regulation of the *R. lignosus* cellulases both by contributing to lignin degradation and by polymerizing toxic lignin-related phenols (20,25,28).

As reported for *Phanerochaete chrysosporium* (39), *R. lignosus* appears to use different types of mechanisms for degrading xylem cell walls in vivo. When wall digestion occurs from the highly lignified middle lamella toward cell lumens, selective delignification probably can be promoted. On the other hand, wall penetration from cell lumens toward primary walls suggests that cellulose, or hemicellulose, may be degraded first. Moreover, microscope observations of sections showing such wall penetration revealed unlabeled areas in which granular material was still present (Fig. 5B). Similar observations also were made within areas of degraded S_1 layers located away from the fungus. At last, two hypotheses can be raised to explain this result.

First, the remaining unlabeled matrix in degraded xylem cell walls may be made of lignin and/or hemicelluloses. Previous work (35) has shown that the enzymatic degradation of xylem cell walls by *R. lignosus* concerns both lignin and polysaccharides. Because extracellular hydrolases of root rot fungi are known to diffuse through wood cell walls (12) and to act far from hyphal tips (16), it is likely that *R. lignosus* digests cellulose first, or simultaneously with lignin, as already shown with some root-rotting fungi (13,37). Other similar pathogens preferentially remove lignin before cellulose depletion (7,9,36–38), whereas few others selectively degrade lignin without a substantial loss of cellulose (6), such as mutants that lack cellulase activity (15,39). In addition, lignin cannot be degraded by white root rot fungi without loss of some carbohydrates from the wood (22,24). Thus, *R. lignosus* may find this required carbon source by digesting cellulose first, or simultaneously with lignin and hemicelluloses.

Second, the remaining material may be cellulose, the susceptibility of which to enzyme degradation was somewhat modified during pathogenesis (i.e., modification in the degree of polymerization or in the degree of crystallinity) as suggested by Goodman et al (23). The nonreducing ends of cellulose might be inaccessible to the exoglucanase-gold complex.

Examination of wood in roots of young artificially-infected dead rubber plants showed that cellulose degradation was irregular throughout xylem cell walls. Large wall areas remain unaltered as indicated by the intense labeling (figure not shown). This raises the question of to what extent the cellulase complex produced by *R. lignosus* (21,27) is involved in pathogenesis. It is likely that cellulases are 1) essential for supplying food for developing hyphae in nonlignified tissues, and 2) necessary for tissue colonization and decay in both phellem and vascular tissues. However, they are probably not key determinants in inducing infected rubber tree death.

Cellulases of *R. lignosus* may strongly contribute to initiate the white rot type of attack, because cellulose degradation was observed in the early stage of root penetration. Moreover, it was observed that initiation of natural tree infection was easier to induce in young plantations, probably because young trees are more susceptible to root rot fungi than adult trees. Natural infection of such trees occurred as early as 12 mo after planting (31), when lignified tissues of roots still were poorly developed. Nevertheless, additional cytochemical investigations are needed to gain a better insight into the role of wall-degrading enzymes secreted by *R. lignosus* in roots of rubber trees, and their role in pathogenesis.

LITERATURE CITED

1. Bartnicki-Garcia, S. 1968. Cell wall chemistry, morphogenesis and taxonomy of fungi. Annu. Rev. Microbiol. 22:87-108.
2. Benhamou, N. 1989. Cytochemical localization of β-(1-4)-D-glucans in plant and fungal cells using an exoglucanase-gold complex. Electron Microsc. Rev. 2:123-138.
3. Benhamou, N., Chamberland, H., Noel, S., and Ouellette, G. B. 1990. Ultrastructural localization of β-1,4-glucan-containing molecules in the cell walls of some fungi: A comparative study between spore and mycelium. Can. J. Microbiol. 36:149-158.
4. Benhamou, N., Chamberland, H., Ouellette, G. B., and Pauzé, F. J. 1987. Ultrastructural localization of β-(1-4)-D-glucans in two pathogenic fungi and in their host tissues by means of an exoglucanase-gold complex. Can. J. Microbiol. 33:405-417.
5. Berg, R. H., Erdos, G. W., Gritzali, M., and Brown, R. D., Jr. 1988. Enzyme-gold affinity labelling of cellulose. J. Electron Microsc. Tech. 8:371-379.
6. Blanchette, R. A. 1984. Screening wood decay by white root rot fungi for preferential lignin degradation. Appl. Environ. Microbiol. 48:647-653.
7. Blanchette, R. A. 1984. Selective delignification of eastern hemlock by *Ganoderma tsugae*. Phytopathology 74:153-160.
8. Blanchette, R. A., Abad, A. R., Cease, K. R., Lovrien, R. E., and Leathers, T. D. 1989. Colloidal gold cytochemistry of endo-1,4-β-glucanase, 1,4-β-D-glucan cellobiohydrolase, and endo-1,4-β-xylanase: Ultrastructure of sound and decay birch wood. Appl. Environ. Microbiol. 55:2293-2301.
9. Blanchette, R. A., Otjen, L., and Carlson, M. C. 1987. Lignin distribution in cell walls of birch wood decayed by white rot basidiomycetes. Phytopathology 77:684-690.
10. Bonfante-Fasolo, P., Vian, B., Perotto, S., Faccio, A., and Knox, J. P. 1990. Cellulose and pectin localization in roots of mycorrhizal *Allium porum:* Labelling continuity between host cell wall and interfacial material. Planta 180:537-547.
11. Chamberland, H., Benhamou, N., Ouellette, G. B., and Pauzé, F. J. 1989. Cytochemical detection of saccharide residues in paramural bodies formed in tomato root cells infected by *Fusarium oxysporum* f. sp. *radicis-lycopersici*. Physiol. Mol. Plant Pathol. 34:131-146.
12. Cowling, E. B. 1961. Comparative biochemistry of the decay of sweetgum sapwood by white rot and brown rot fungi. U.S.D.A. Tech. Bull. 1258.
13. Daniel, G., Nilsson, T., and Pettersson, B. 1989. Intra- and extracellular localization of lignin peroxidase during the degradation of solid wood and wood fragments by *Phanerochaete chrysosporium* by using transmission electron microscopy and immuno-gold labeling. Appl. Environ. Microbiol. 55:871-881.
14. D'Auzac, J., Jacob, J. L., and Chrestin, H. 1989. Physiology of Rubber Tree Latex. CRC Press, Boca Raton, FL.
15. Eriksson, K. E. 1981. Fungal degradation of wood components. Pure Appl. Chem. 53:33-43.
16. Eriksson, K. E., and Wood, T. M. 1985. Biodegradation of cellulose. Pages 469-503 in: Biosynthesis and Biodegradation of Wood Components. T. Higuchi, ed. Academic Press, New York.
17. Esau, K. 1977. Periderm. Pages 183–197 in: Anatomy of Seed Plants. 2nd ed. John Wiley & Sons, New York.
18. Frens, G. 1973. Controlled nucleation for regulation of the particule size in monodisperse gold suspensions. Nature Phys. Sci. 241:20-22.
19. Galliano, H., Gas, G., and Boudet, A. M. 1988. Biodegradation of *Hevea brasiliensis* lignocelluloses by *Rigidoporus lignosus:* Influence of culture conditions and involvement of oxidizing enzymes. Plant Physiol. Biochem. 26:619-627.
20. Geiger, J. P., Huguenin, B., Nicole, M., and Nandris, D. 1986. Laccases of *Rigidoporus lignosus* and *Phellinus noxius*. II. Effects of *R. lignosus* laccase L1 on thioglycolic lignin of *Hevea*. Appl. Bio-

chem. Biotechnol. 13:97-111.
21. Geiger, J. P., Nicole, M., Nandris, D., and Rio, B. 1986. Root rot diseases of *Hevea brasiliensis*. I. Physiological and biochemical aspects of root aggression. Eur. J. For. Pathol. 16:22-36.
22. Geiger, J. P., Rio, B., Nicole, M., and Nandris, D. 1986. Biodegradation of *Hevea brasiliensis* wood by *Rigidoporus lignosus* and *Phellinus noxius*. Eur. J. For. Pathol. 16:147-159.
23. Goodman, R. N., Kiraly, Z., and Wood, K. R. 1986. The biochemistry and physiology of plant disease. University of Missouri Press, Columbia.
24. Kirk, T. K., Connors, W. T., and Zeikus, J. G. 1976. Requirement of a growth substrate during lignin decomposition by two wood rotting fungi. Appl. Environ. Microbiol. 32:192-194.
25. Kirk, T. K., and Shimida, M. 1985. Lignin biodegradation: The microorganisms involved, and the physiology and the biochemistry of degradation by white root rot fungi. Pages 579-605 in: Biosynthesis and Biodegradation of Wood Components. T. Higuchi, ed. Academic Press, New York.
26. Kolattukudy, P. E. 1980. Biopolyester membranes of plants: Cutin and suberin. Science 208:990-1000.
27. Lafitte, M., Barthe, J. P., and Touzé, A. 1988. Production d'hydrolases dégradant des polyosides pariétaux par *Rigidoporus lignosus,* un des agents du pourridié blanc de l'Hévéa. Eur. J. For. Pathol. 18:1-7.
28. Lewis, N. G., and Yamamoto, E. 1990. Lignin: Occurrence, biogenesis and biodegradation. Annu. Rev. Plant Physiol. Plant Mol. Biol. 41:455-496.
29. Nandris, D., Nicole, M., and Geiger, J. P. 1983. Infections artificielles de jeunes plants d'*Hevea brasiliensis* par *Rigidoporus lignosus* et *Phellinus noxius*. Eur. J. For. Pathol. 13:65-76.
30. Nandris, D., Nicole, M., and Geiger, J. P. 1987. Root rot diseases of rubber trees. Plant Dis. 71:298-306.
31. Nandris, D., Nicole, M., Geiger, J. P., and Mallet, B. 1983. Root rot diseases in the forests and plantations of the Ivory Coast. Pages 286-295 in: Proc. Intl. Conf. Root Rot and Butt Rots of Forest Trees, 6th, Melbourne.
32. Nicole, M., Geiger, J. P., and Nandris, D. 1986. Penetration and degradation of suberized cells of *Hevea brasiliensis* infected with root rot fungi. Physiol. Mol. Plant Pathol. 28:181-185.
33. Nicole, M., Geiger, J. P., and Nandris, D. 1986. Root rot diseases of brasiliensis. II. Some host reactions. Eur. J. For. Pathol. 16:37-55.
34. Nicole, M., Geiger, J. P., and Nandris, D. 1986. Ultrastructure of laticifer modifications in *Hevea brasiliensis* infected with root rot fungi. J. Phytopathol. 116:259-268.
35. Nicole, M., Geiger, J. P., and Nandris, D. 1987. Ultrastructural aspects of rubber tree root rot diseases. Eur. J. For. Pathol. 17:1-10.
36. Otjen, L., and Blanchette, R. A. 1986. Selective delignification of birch wood (*Betula papyrifera*) by *Hirschioporus pargamenus* in the field and laboratory. Holzforschung 40:183-189.
37. Otjen, L., Blanchette, R. A., Effand, M. J., and Leatham, G. F. 1987. Assessment of 30 white rot basidiomycetes for selective lignin degradation. Holzforschung 41:343-349.
38. Ruel, K., and Barnoud, F., 1985. Degradation of wood by microorganisms. Pages 441-467 in: Biosynthesis and Biodegradation of Wood Components. T. Higuchi, ed. Academic Press, New York.
39. Ruel, K., Barnoud, F., Joseleau, J. P., Johnrusd, S. C., and Eriksson, K. E. 1986. Ultrastructural aspects of birch wood degradation by *Phanerochaete chrysosporium* and two of its cellulase deficient mutants. Holzforschung 40:5-9.